Study of 5-nitroindazoles' anti-*Trypanosoma cruzi* mode of action: Electrochemical behaviour and ESR spectroscopic studies

Jorge Rodríguez [a,b], Alejandra Gerpe [c], Gabriela Aguirre [c], Ulrike Kemmerling [d], Oscar E. Piro [e], Vicente J. Arán [f], Juan Diego Maya [d], Claudio Olea-Azar [a,*], Mercedes González [c,**], Hugo Cerecetto [c,**]

[a] *Departamento de Química Inorgánica y Analítica, Facultad de Ciencias Químicas y Farmacéuticas, Universidad de Chile, Santiago, Chile*
[b] *Departamento de Química, Facultad de Ciencias Básicas, Universidad Metropolitana de Ciencias de la Educación, Santiago, Chile*
[c] *Departamento de Química Orgánica, Facultad de Ciencias/Facultad de Química, Universidad de la Republica, Montevideo, Uruguay*
[d] *Departamento de Farmacología Molecular y Clínica, Facultad de Medicina, Universidad de Chile, Santiago, Chile*
[e] *Departamento de Física, Facultad de Ciencias Exactas, Universidad Nacional de La Plata and Instituto IFLP (CONICET), C.C. 67, 1900 La Plata, Argentina*
[f] *Instituto de Química Médica (CSIC), Juan de la Cierva, 3, 28006 Madrid, Spain*

A B S T R A C T

New indazole derivatives have been developed to know about structural requirements for adequate anti-*Trypanosoma cruzi* activity. In relation to position 1 of indazole ring, we have observed that a butylaminopentyl substituent (**14**) affords good activity, but *N*-oxidation of ω-tertiary amino moiety yields completely inactive compounds (**17**, **18**); the substituent at position 3 of indazole ring affects drastically the *in vitro* activity, 3-OH derivative **13** being completely inactive. On the other hand, since compound **22**, denitro-analogue of active compound **4**, does not show activity, the 5-nitro substituent of indazole ring seems to be essential. Intramolecular cyclization of side chain at position 1 also affords inactive compounds (**19**, **20**). The electrochemical studies showed that the trypanocidal 5-nitroindazole derivatives yielded nitro-anion radical via one-electron process at physiological pH. This electrochemical behaviour occurs in the parasite according to ESR experiment with the *T. cruzi* microsomal fraction showing that 5-nitroindazole derivatives suffer bio-reduction without reactive oxygen species generation.

Keywords:
5-Nitroindazole
Anti-*T. cruzi* agents
Mode of action

1. Introduction

American trypanosomiasis or Chagas' disease, in which we have centered the present study, has like etiological agent the *Trypanosoma cruzi*, protozoan parasite with complex life cycle, endemic of Latin America. Latest data from the WHO indicates that over 24 million people are infected or at least serologically positive for *T. cruzi* [1]. Currently, this pathology is treated with nitroheterocyclic agents such as nifurtimox (Nfx) and benznidazole (Bnz) [2]. Both display effectiveness similar in the acute and undetermined phases of this disease, but the latter is preferred due to its simpler administration and that it shows less severe secondary effects; in fact, Nfx has been retired from the market in many countries. It is believed that they act through a bio-reduction of the NO_2 group, but their mechanisms of action are different [3,4]. Different therapeutic targets are currently being studied but it does not appear that any drugs could replace Nfx and Bnz. Therefore, the search for new and better drugs against *T. cruzi* is of paramount importance.

Despite their toxicity, nitroaromatic compounds are generally very potent against *T. cruzi* and have been considered as important hits for molecular modifications [5,6]. We had previously described the *in vitro* anti-*T. cruzi* activity of some 5-nitroindazole derivatives, i.e. **1**–**7** (Scheme 1), some of them having remarkable anti-epimastigote properties, and displaying also certain antineoplastic activity that confirms the previously observed parallelism between

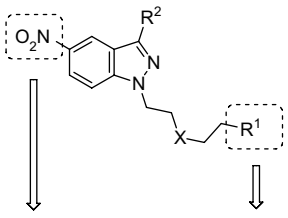

-X-	-R^1	-R^2	Compound
-O-	-dimethelylamine	-OH	**1**
-O-	-piperidino	-OH	**2**
-O-	-piperidino	-OCH_3	**3**
-CH_2-	-dimethelylamine	-OBn	**4**
-O-	-dimethelylamine	-OBn	**5**
-CH_2-	-piperidino	-OBn	**6**
-O-	-piperidino	-OBn	**7**

Scheme 1.

* Corresponding author. Fax: +56 2 7370567.
** Corresponding authors.
E-mail address: colea@uchile.cl (C. Olea-Azar).

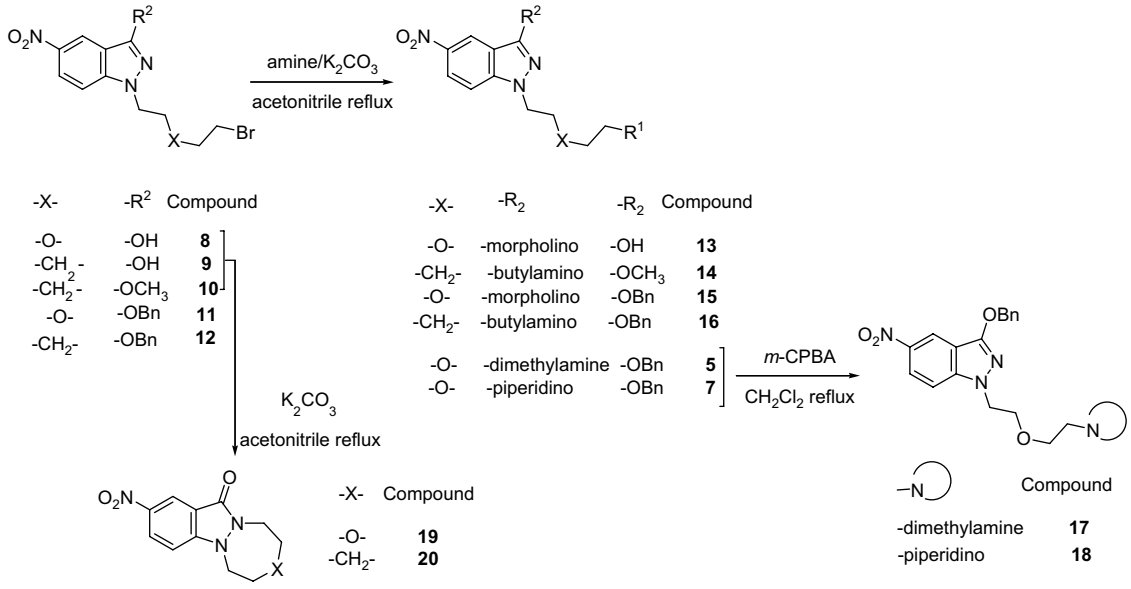

Scheme 2.

antichagasic and anticancer activities [7a]. Interestingly, some of these 5-nitroindazoles did not show significant unspecific cytotoxicity against macrophages [7a].

Recently, we have also demonstrated the effectiveness in an *in vivo* acute model of Chagas disease of the 5-nitroindazoles **3** and **5** (Scheme 1) [7b]. In order to observe the chemoprophylactic effects of these derivatives we tested the anti-trypomastigote (CL Brener clone) activity in blood presenting derivatives **3**–**5** (Scheme 1) remarkable activities at a dose of 250 μg mL [7b]. In this first approach it was done mainly modifications at the lateral chain in 1- and 3-positions by varying –X–, $-R^1$ and $-R^2$ (see Scheme 1). Some theoretical and experimental physicochemical studies were done in order to understand the mode of trypanocidal action of these compounds, however, some structural modifications and deep studies on mechanism of action would be performed [7a,8].

Herein, we describe the synthesis of new 5-nitroindazoles modifying mainly the substitution in R^1, including lipophilic and hydrophilic amino-substituents, the flexibility in backbone at the 1-position and avoiding the presence of the nitro moiety at the 5-position (Scheme 1). We also describe the anti-*T. cruzi* activities. The performed structural modifications together with electrochemical and ESR studies allow us to get inside the mechanism of action.

2. Methods and results

2.1. Synthesis

Three different modifications at the level of R^1 substituent were done: inclusion of a lipophilic amino substituent (thiomorpholino moiety), hydrophilic amino substituent (*N*-oxide of amino moiety), and donor hydrogen-bond amino substituent (butylamino moiety). These derivatives were prepared following the pathways shown in Scheme 2. Using bromides **8**–**12** as common starting materials, the reaction with thiomorpholine or butylamine in the presence of potassium carbonate afforded derivatives **13**–**16** in good yields [7]. In reference to the *N*-oxidation of amino-substituents in the lateral chain, *m*-chloroperbenzoic acid was used successfully generating regio-selectively products **17** and **18** (Scheme 2), without oxidation of indazole nitrogen atoms. On the other hand, the derivatives treated with urea–hydrogen peroxide complex, in the presence of trifluoroacetic acid, were assayed unsuccessfully obtaining the de-benzylated derivatives **1** and **2** (Scheme 1), as main reaction products. For the generation of a backbone in 1-position with restricted mobility, reactants **8** and **9** were cyclized in the presence of potassium carbonate in acetonitrile at reflux to afford the corresponding fused indazolinones **19** and **20** (Scheme 2) [9]. The generation of a derivative lacking the 5-nitro substituent, was assayed unsuccessfully for the reduction of the nitro group, in the presence of Fe/HCl (Scheme 3)a, to generate intermediate **21**. However, in these conditions the complexation of indazole system took place without generation of the desired amine **21**. Consequently, we assayed the synthetic procedure shown in Scheme 3b starting from 3-hydroxy-1*H*-indazole **23** and affording the desired derivative **22**, 5-denitro-analogue of active compound **4**, in good global yield [10–13]. All new compounds were characterized by NMR (^{1}H, ^{13}C, HMQC, and HMBC), MS and IR analyses and their purity was established by TLC and microanalysis. Single crystals of derivative **13** adequate for structural X-ray diffraction studies[1] were

[1] (a) In derivative **13** the 5-nitro group is nearly coplanar with the indazole ring. As expected, intramolecular distances within the phenyl ring correspond to a delocalized bond structure [C–C bond lengths in the range from 1.373(3) to 1.404(3) Å]. Within the fused heterocycle ring the double C4–N2 bond distance is 1.311(2) Å, significantly shorter (13σ) than single C5–N3 bond length [1.338(2) Å] and single C8–N3 bond distance [1.452(2) Å]. The 4-thiomorpholine ring is folded back onto the fused ring group and shows a single bonded chair conformation. C–C distances are 1.510(3) and 1.517(2) Å; C–N distances are equal to each other [1.480(2) Å]; S–C bond lengths are also equal to each other within experimental accuracy [1.800(3) Å]. The molecules are arranged in the lattice as centrosymmetric dimers where the hydroxyl group of a monomer forms a strong O–H···N bond with the 4-thiomorpholine N-atom of an inversion related molecule [d(O3···N4) = 2.592 Å, d(H3···N4) = 1.435 Å, ∠(O3–H3···N4) = 165.2°]. Fractional atomic coordinates and equivalent displacement parameters, full bond distances and angles, anisotropic displacement parameters along with detailed crystal data, data collection procedure, structure determination method and refinement results are given as Supporting information. (b) Enraf-Nonius (1997–2000). COLLECT. Nonius BV, Delft, The Netherlands. (c) K. Harms, S. Wocadlo, XCAD4 – CAD4 Data Reduction, University of Marburg, Marburg, Germany, 1995. (d) PLATON, A Multipurpose Crystallographic Tool, Utrecht University, Utrecht, The Netherlands, A.L. Spek, 1998. (e) G.M. Sheldrick, *SHELXS-97. Program for Crystal Structure Resolution*. University of Göttingen: Göttingen, Germany, 1997. (f) G.M. Sheldrick, *SHELXL-97. Program for Crystal Structures Analysis*. University of Göttingen: Göttingen, Germany, 1997. (g) C. K. Johnson, ORTEP-II. A Fortran Thermal-Ellipsoid Plot Program. Report ORNL-5138, Oak Ridge National Laboratory, Tennessee, USA, 1976.

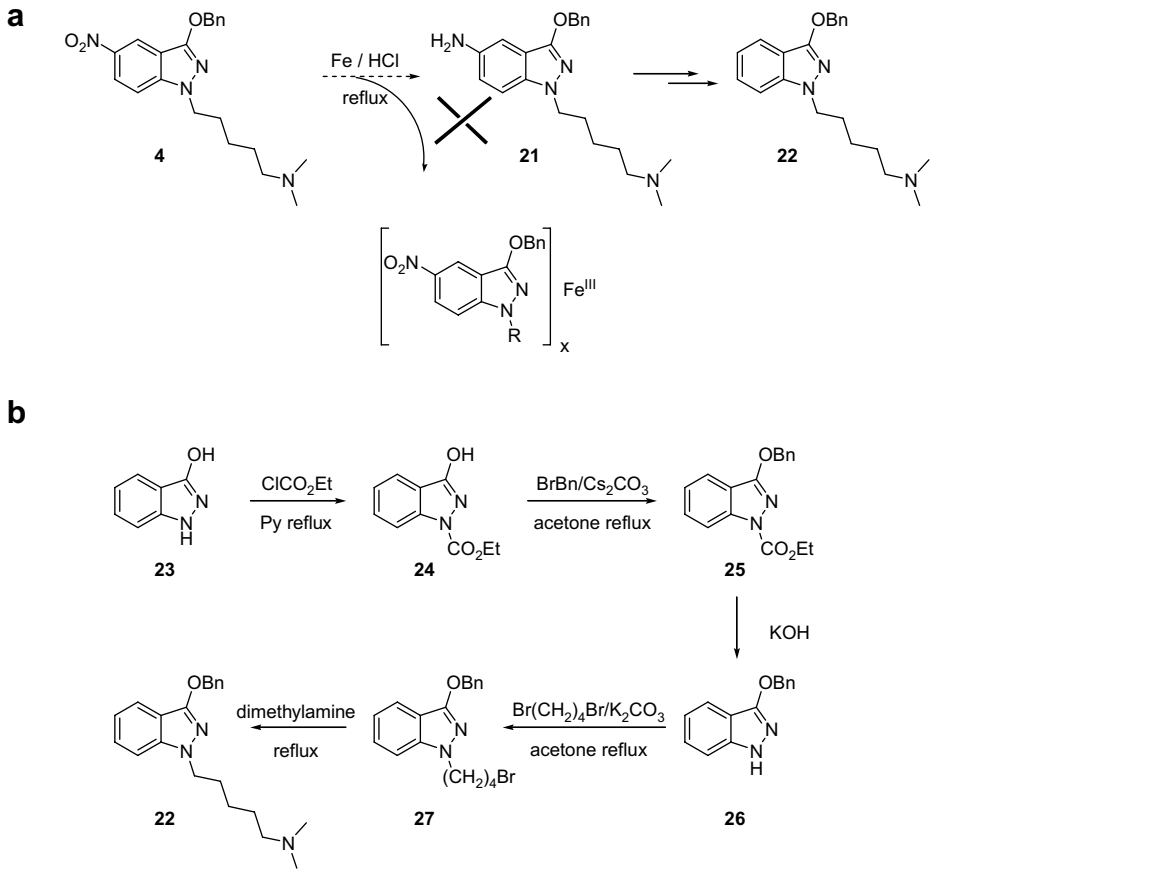

Scheme 3.

obtained by slow evaporation from an EtOH solution. Fig. 1 shows the ORTEP molecular drawing of derivative **13**.

In order to study the preferential conformation of these derivatives in solution, two-dimensional rotating frame nuclear Overhauser effect spectroscopy (ROESY) experiments were carried out in DMSO. An expansion of the ROESY spectrum of derivative **13** is shown in Fig. 2. The inspection of the ROESY spectra allowed the establishment of spatial proximities between several aromatic hydrogens of the indazole moiety and the lateral chain protons. The two-dimensional spectrum shows several intramolecular cross-peaks, i.e. between 7*H*-indazole and 5′*H*-lateral chain protons, high intensity cross-peaks, 7*H*-indazole and 4′*H*- and 2′H-lateral chain protons of the lateral chain and 6*H*-indazole and 5′H-lateral chain protons, and less intense cross-peaks. These results indicate that the 3-oxapentyl lateral chain could be in a folded conformation wherein the major cross-peak is between 7*H* and 5′*H* protons. Furthermore, cross-peaks does not appear between the protons of the lateral chain and 4*H* proton of indazole moiety indicating some preferential folding in solution that involves only 6*H*- and 7*H*-indazole protons. This result is in agreement with the distribution in solid state.

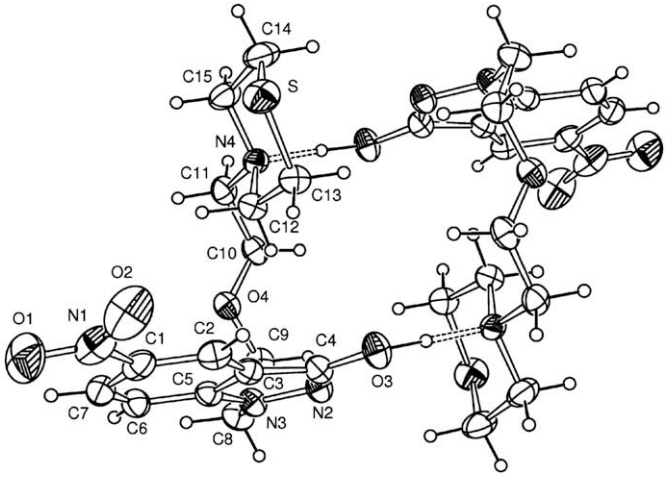

Fig. 1. Derivative **13**-dimer molecular graphic displaying the numbering of molecular structure. Displacement ellipsoids are drawn at the 30% probability level.

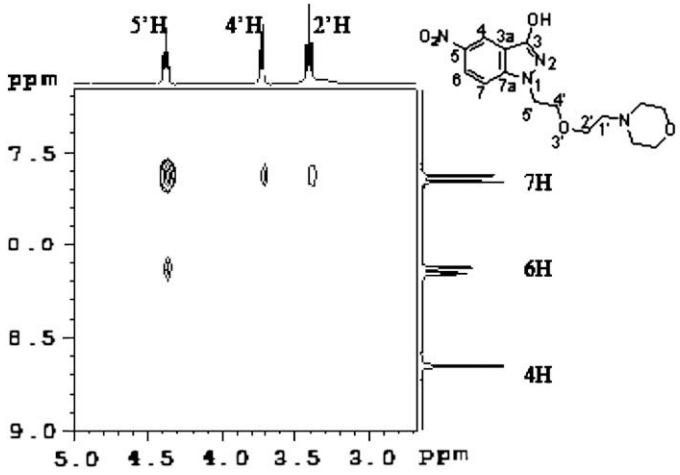

Fig. 2. Partial contour plot of the two-dimensional ROESY spectrum of derivative **13** in DMSO-d_6.

2.2. Biological characterization: anti-trypanosomal activity

All the compounds were tested *in vitro* against CL Brener clone of epimastigote forms of *T. cruzi* at different concentrations. Table 1 shows the percentage of growth inhibition (% GI) of the indazole derivatives at 25 μM. The most active of the new indazole derivatives was **16** with IC_{50} value in the same order as that of the reference drug (Nfx), while compound **14** showed medium activity at the assayed concentration.

The most active 5-nitroindazole derivatives **4**–**6**, **14**, and **16** (Table 1) and Nfx were tested upon non-replicative trypomastigote forms of the parasite. These forms are found in mammalian blood and are the target for antichagasic drugs. A viability test such as MTT reduction was carried out using drug concentrations equivalent to IC_{50} values for epimastigotes. The value of viabilities (Table 2) ranged from 0 to 40% compared with untreated control. The new derivative **14** displayed similar activity of that of Nfx while parent compounds **4**–**6** and the new developed derivative **16** showed stronger activity against trypomastigote-*T. cruzi* than Nfx. This result confirms the trend observed upon epimastigote forms and previously reported trypomastigote activities and *in vivo* activities found for these 5-nitroindazole derivatives.

2.3. Study of anti-T. cruzi mechanism of action

In order to study if oxidative stress mediates the biological action of these derivatives we performed some experiments related to this fact. We studied the indazoles' electrochemical behaviour in protic media and the indazoles' production of free radicals into the parasite, by ESR experiments.

2.3.1. Electrochemical behaviour

Electrochemical behaviour in protic media for this family of indazole derivatives was studied using buffer Britton–Robinson/EtOH (70:30) adjusting to pH 2.0, 7.1 and 9.0. A hanging mercury drop electrode was used as the working electrode. Fig. 3a shows the cyclic voltammogram obtained at pH 2.0 when a solution of derivate **14** was electrolyzed. Two irreversible reduction peaks are observed, a first peak around −0.4 V could correspond to the electroreduction of the nitro group (Ic) by four electrons, to form the hydroxylamine derivative, similar to the results previously observed for other 5-nitroimidazole derivatives in protic medium at the same pH (Eq. (1)) [14]. The second irreversible peak was displayed at more negative potential around −0.8 V (IIc), which corresponds to the electroreduction of the protonated hydroxylamine group to form the corresponding amino derivative. The hydroxylamine group generated in the nitro-reduction could accept one or two protons and both the mono- and the diprotonated forms could undergo reduction at potentials more negative than the corresponding nitro group [15]. In this media, such reduction occurs in a two-electron step (see Eq. (2)). At higher pH values, usually at pH greater than about 4, the height of this wave decreases with increasing pH and at pH > 6, physiological pH, virtually no reduction is observed [15]. The decrease reflects the decrease in rate of protonation with increasing pH. Fig. 3b shows the results at pH 7 observing that the reductive peak (IIc), corresponding to the formation of amino derivative, disappears. Hydroxylamine derivative formed is a highly reactive species, which could undergo numerous chemical and electrochemical reactions. In our case, it could be electrooxidized to the corresponding nitroso derivative. At pH 7 it is possible to observe in the voltammogram a reversible couple (IVa/IVc) which appears at sufficiently low potential, −0.10 V corresponding to the reversible reduction of nitroso derivative that was formed by electrooxidation of the hydroxylamine derivative. In this reversible couple, the cathodic peak appears only after the accumulation of at least one cyclic voltammogram indicating that the step is hydroxylamine oxidation dependent. The nature of the peaks was recognized early by nitrobenzene (Eq. (3)) [15,16].

$$R{-}NO_2 + 4e^- + 4H^+ \rightarrow R{-}NHOH + H_2O \quad (1)$$

$$R{-}NHOH_2^+ + 2e^- + H^+ \rightarrow R{-}NH_2 + H_2O \quad (2)$$

$$R{-}NHOH \leftrightarrow R{-}NO + 2e^- \quad (3)$$

On the other hand, during the reduction at physiological pH (Fig. 3b) it was possible to note that the peak (Ic) corresponding to the nitro group four-electron reduction wave is split into two peaks (Ic and IIIc), which suggests that in neutral and alkaline solutions the four-electron reduction occurs in two separate steps. The one-electron reduction from $R{-}NO_2$ to $R{-}NO_2^{\bullet -}$ (nitro-anion radical) (Ic) (Eq. (4)) precedes the three-electron reduction process (wave IIIc) (Eq. (5)). Both reduction waves are shifted to more negative potentials, −0.56 and −1.41 V, respectively. These results show that $R{-}NO_2^{\bullet -}$ radical anion is stabilized in neutral and alkaline media. Previous reports show similar results for cyclic voltammetry of nitrobenzene in alkaline medium on Au electrode [15,16].

$$R{-}NO_2 + e^- \rightarrow R{-}NO_2^{\bullet -} \quad (4)$$

$$R{-}NO_2^{\bullet -} + 3e^- + 4H^+ \rightarrow R{-}NHOH + H_2O \quad (5)$$

Table 1
In vitro antichagasic activity of indazole derivatives

Compound	% GI[a,b] (IC_{50}, μM)
1	3[c]
2	9[c]
3	25[c]
4	100 (12.5)[c]
5	80 (16.4)[c]
6	100 (6.6)[c]
7	24[c]
13	0
14	58 (22.0)
15	20
16	94 (11.0)
17	0
18	6
19	6
20	4
22	18
Nfx	100 (3.4)

[a] Values expressed as percentage of inhibition of control growth (% GI). Compounds tested at 25 μM concentration.
[b] Results are the means of three different experiments with SD less than 10% in all cases.
[c] From Ref. [7].

Table 2
Effect of 5-nitroindazole derivatives upon *T. cruzi* trypomastigote viability after 24 h treatment

Compound	Viability[a]
4	0.49 ± 0.007
5	0.56 ± 0.003
6	0.29 ± 0.007
14	40.04 ± 0.100
16	−0.37 ± 0.005
Nfx	50.89 ± 0.058

[a] Drug concentrations used were the IC_{50} obtained from epimastigote form of *T. cruzi* (CL Brener clone, Table 1). For details see Section 5.

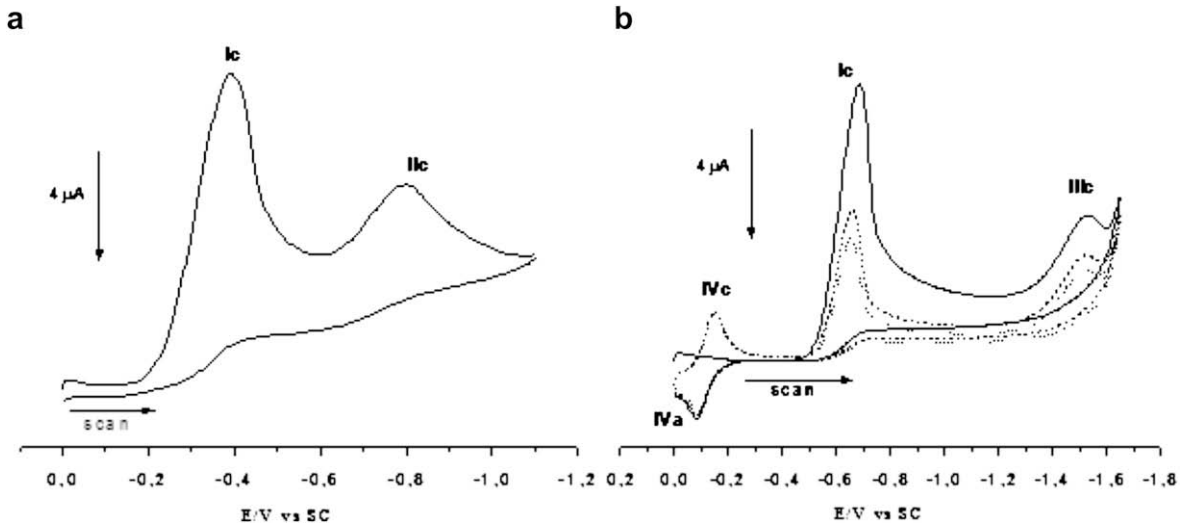

Fig. 3. (a) Derivative **14** (1 mM) cyclic voltammogram in protic media (buffer Britton–Robinson/EtOH 70:30 + 0.1 M KCl), pH 2.0, speed 2.0 V s^{-1}. (b) Derivative **14** (1 mM) cyclic voltammogram in protic media (buffer Britton–Robinson/EtOH 70:30 + 0.1 M KCl), pH 7.1, speed 2.0 V s^{-1}.

On the other hand, previous reports had indicated that C═N indazole moiety reduction takes place at high reduction potentials, around 1.6 V, in protic medium [17,18]. Nevertheless, when a solution of derivative **22** was used in the electrochemical studies, this was not electrolyzed under our work conditions. This result indicates that in our conditions the nitro group is the only electroactive species in 5-nitroindazole derivatives. In addition, the same behaviour was obtained for 5-nitroindazolone derivatives **19** and **20**.

2.3.2. ESR spectroscopic studies

In order to analyse the capacity of these compounds to generate free radicals into the parasite we incubated our derivatives with *T. cruzi* microsomes in the presence of NADPH, and the spin trapping DMPO [19–22]. Fig. 4 shows the ESR spectrum obtained when DMPO was added to the system **14**–*T. cruzi* microsomes, this spectrum being in agreement with the trapped nitro-anion radical species which is generated from the nitro-bio-reduction. The six lines have the following hyperfines $a_N = 15.95$ G and $a_H = 23.00$ G consistent with the trapped nitro-anion radical (marked with * in Fig. 4c). Moreover, these results could be indicating that the mode of action of these derivatives does not stimulate, unlike Nfx, the superoxide, hydroxyl radical or hydrogen peroxide generation [23,24]. However, it makes evident the presence of 5-nitroindazole reduced metabolites, which could be probably involved in its trypanocidal activity showing a mechanism of action similar to that of benznidazole [25–27].

3. Discussion

The newly developed 5-nitroindazole derivatives allow us to extract some structural requirements for adequate trypanocidal

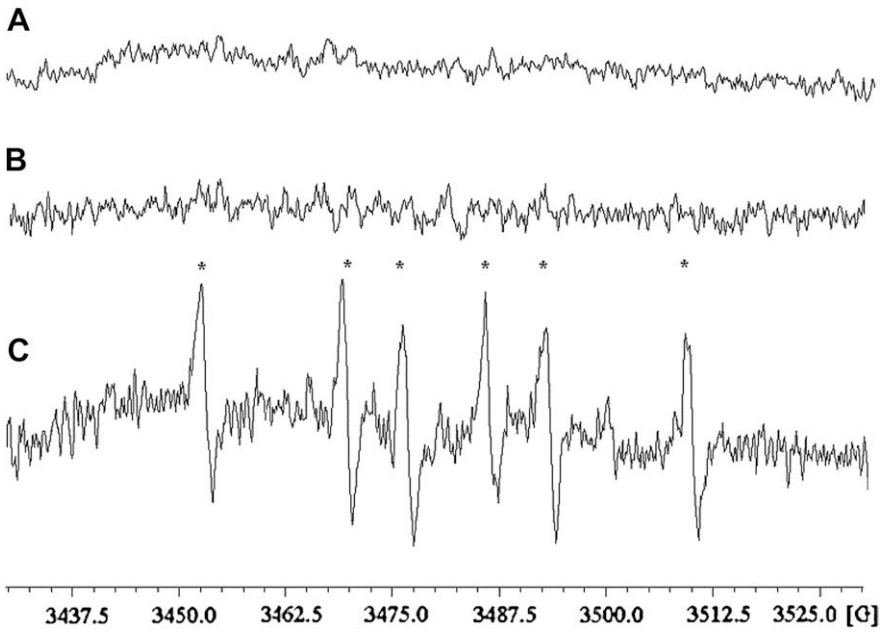

Fig. 4. ESR spectra of DMPO–**14** radical adducts obtained with *T. cruzi* microsomes. The ESR spectra were observed 25 min after incubation at 28 °C with *T. cruzi* microsomal fraction (4 mg protein/mL), NADPH (1 mM), in phosphate buffer (20 mM), pH 7.4 (A) DMSO (10 v/v) and DMPO (100 mM), (B) **14** (1 mM in DMSO 10 v/v) and (C) **14** (2 mM in DMSO 10 v/v) and DMPO (100 mM). Spectrometer conditions: microwave frequency 9.75 GHz, microwave power 20 mW, modulation amplitude 0.87 G, time constant 0.25 s, number of scans 10.

activity. The kind of indazole 3-substituent affects drastically the *in vitro* activity, producing 3-OH substituent a complete loss of activity and 3-OBn substituent the most active compounds in each series of analogues (compare activity of derivatives **13** and **15**, or parent compounds **1** and **5**). The change of piperidino substituent by a thiomorpholino moiety does not improve the activity (compare activity of derivative **15** and parent compound **7**); however, if the change is by a butylamino substituent the activity increases (compare activity of derivative **14** and parent compound **3**). Neither the *N*-oxidation of amino substituent in indazole at the 1-position (compare activity of derivative **17** and parent compound **7**, or derivative **18** and parent compound **5**) nor the cyclization (derivatives **19** and **20**) produces an improvement in the trypanocidal activity. The absence of the 5-nitro moiety produces a loss of activity (compare activity of derivative **22** and parent compound **4**).

The electrochemical studies, in protic media and different pH, showed different reduction behaviour of the trypanocidal 5-nitroindazole derivatives, yielding hydroxylamine via a single four-electron reduction at pH 2.0 and nitro-anion radical via one-electron process at physiological pH (7.1). In these conditions, the final hydroxylamine derivative formed was electrooxidized to the corresponding nitroso-analogue. This electrochemical behaviour occurs into the parasite according to ESR experiment with the *T. cruzi* microsomal fraction showing that 5-nitroindazole derivatives suffer bio-reduction without reactive oxygen species generation. However, in spite of that electrochemical characteristics are similar for all family, we believe that other factors would affect behaviour in the biological activities. The reduction mechanism could be different in biological system. On the other hand, the structural features of the 5-NI derivatives revealed a mimetic similarity with non-peptide inhibitors represented by the tricyclic ring structures which are competitive inhibitors of trypanothione reductase (TR). The tricyclic moiety of these compounds was shown to lodge against the hydrophobic wall of TR active site [33]. In addition, the presence of protonatable amino groups in a long alkylamino chain is indispensable for TR recognition. In this sense, the trypanocidal activity observed could be the result of a mixed mechanism that considers the bio-reduction and an uncompetitive inhibitor of TR.

4. Conclusion

The results presented above indicate that 5-indazole system constitutes a start point for further drug development. The mechanism of action proves to be related to the production of reduced species of the nitro moiety similar to that observed with Bnz. The results provide supporting evidence to stimulate further *in vivo* studies of the new compounds in appropriate animal models of Chagas' disease.

5. Experimental

5.1. Chemistry

Compounds **1**–**12** and **26** were prepared according to literature procedures [7a,12,13]. All starting materials were commercially available research-grade chemicals and used without further purification. All solvents were dried and distilled prior to use. All the reactions were carried out in a nitrogen atmosphere. ^{1}H NMR (300 or 400 MHz) and ^{13}C NMR (75 or 100 MHz) spectra were recorded on a Varian Unity 300, Varian Inova 400 or Bruker DPX-400 spectrometers. The chemical shifts are reported in parts per million from TMS (δ scale). *J* values are given in hertz. The assignments have been performed by means of different standard homonuclear and heteronuclear correlation experiments (ROESY, HMQC and HMBC). Electron impact (EI) mass spectra were obtained at 70 eV on a Shimadzu GC–MS QP 1100 EX instrument. IR spectra were recorded on a Perkin Elmer 1310 spectrometer, using potassium bromide tablets; the frequencies are expressed in cm^{-1}. DC-Alufolien silica gel 60 PF254 (Merck, layer thickness 0.2 mm) and silica gel 60 (Merck, particle size 0.040–0.063 mm) were used for TLC and flash column chromatography, respectively. Elemental analyses were obtained from vacuum-dried samples (over phosphorous pentoxide at 3–4 mm Hg, 24 h at room temperature) and performed on a Fisons EA 1108 CHNS-O analyser.

5.2. N-*[5-(3-Hydroxy-5-nitro-1*H*-indazol-1-yl)-3-oxapentyl]thiomorpholine (**13**)*

A mixture of **8** (1.03 g, 3.1 mmol) and thiomorpholine (1.03 mL, 6.2 mmol) in acetonitrile was heated at reflux for 32 h. The obtained suspension was allowed to stand at 4 °C overnight and then the crystallized tertiary amine was collected by filtration, washed with cold ethanol and air dried, 1.04 g (95%). ^{1}H NMR (400 MHz, DMSO-d_6) δ ppm: 2.34 (2H, t, $J = 5.6$ Hz), 2.44 (8H, m), 3.30 (1H, br), 3.41 (2H, t, $J = 5.6$ Hz), 3.74 (2H, t, $J = 5.0$ Hz), 4.38 (2H, t, $J = 5.0$ Hz), 7.64 (1H, d, $J = 9.6$ Hz), 8.14 (1H, dd, $J = 2.0$, 9.6 Hz), 8.65 (1H, d, $J = 2.0$ Hz); ^{13}C NMR (100 MHz, DMSO-d_6) δ ppm: 27.90, 49.09, 55.52, 58.55, 69.25, 69.46, 111.27, 112.34, 119.29, 122.22, 140.64, 143.68, 157.37. MS (EI): *m*/*z* (%) 352 (M$^+$, 6), 278 (34), 149 (100), 116 (59), 91 (34), 69 (47), 57 (54). Anal. ($C_{15}H_{20}N_4O_4S$) C, 51.12; H, 5.72; N, 15.90; S, 9.10.

5.3. General method for the preparation of **14**–**16**

A mixture of the corresponding bromide (**10**, **11** or **12**, 1 equiv), the corresponding amine (thiomorpholine or butylamine, 2 equiv) and potassium carbonate (2 equiv) was heated at reflux for 21 h (for **14**) or 14 h (for **15** and **16**). After that, the mixture was evaporated to dryness and treated with aqueous potassium carbonate (5%, 30 mL) and dichloromethane (3 × 30 mL). The combined organic layers were dried ($MgSO_4$) and evaporated to dryness to obtain the desired tertiary amines as the corresponding free bases.

5.3.1. N-*[5-(3-Methoxy-5-nitro-1*H*-indazol-1-yl)pentyl]butylamine (**14**)*

Yield: 96%. ^{1}H NMR (400 MHz, $CDCl_3$) δ ppm: 0.93 (3H, t, $J = 7.4$ Hz), 1.40 (4H, m), 1.94 (6H, m), 2.93 (4H, m), 4.11 (3H, s), 4.21 (2H, t, $J = 6.9$ Hz), 7.35 (1H, d, $J = 9.3$ Hz), 8.23 (1H, dd, $J = 2.1$, 9.3 Hz), 8.62 (1H, d, $J = 2.1$ Hz), 9.38 (1H, br); ^{13}C NMR (100 MHz, $CDCl_3$) δ ppm: 13.85, 20.48, 24.42, 25.57, 28.17, 29.12, 47.62, 47.84, 48.61, 56.95, 109.07, 112.13, 119.08, 123.04, 141.24, 143.14, 158.73. MS (EI): *m*/*z* (%) 334 (M$^+$, 1), 319 (44), 246 (46), 206 (43), 160 (22), 98 (50), 86 (100). Anal. ($C_{17}H_{26}N_4O_3$) C, 61.06; H, 7.84; N, 16.75.

5.3.2. N-*[5-(3-Benzyloxy-5-nitro-1*H*-indazol-1-yl)-3-oxapentyl]thiomorpholine (**15**)*

Yield: 90%. ^{1}H NMR (400 MHz, $CDCl_3$) δ ppm: 2.49 (2H, t, $J = 5.6$ Hz), 2.60 (5H, m), 3.49 (2H, t, $J = 5.6$ Hz), 3.87 (2H, t, $J = 5.2$ Hz), 4.40 (2H, t, $J = 5.2$ Hz), 5.46 (2H, s), 7.43 (6H, m), 8.24 (1H, dd, $J = 2.0$, 9.2 Hz), 8.69 (1H, d, $J = 2.0$ Hz); ^{13}C NMR (100 MHz, $CDCl_3$) δ ppm: 28.03, 49.68, 55.55, 58.78, 69.41, 69.85, 71.50, 109.78, 112.00, 118.87, 122.76, 128.54, 128.77, 128.98, 136.61, 141.38, 141.40, 144.00, 158.08. MS (EI): *m*/*z* (%) 442 (M$^+$, 1), 351 (7), 129 (22), 116 (100), 91 (37). Anal. ($C_{22}H_{26}N_4O_4S$) C, 59.71; H, 5.92; N, 12.66; S, 7.25.

5.3.3. N-*[5-(3-Benzyloxy-5-nitro-1*H*-indazol-1-yl)pentyl]butylamine (**16**)*

Yield: 95%. ^{1}H NMR (400 MHz, $CDCl_3$) δ ppm: 0.92 (3H, t, $J = 7.4$ Hz), 1.39 (4H, m), 1.86 (6H, m), 2.89 (4H, m), 4.22 (2H, t, $J = 6.9$ Hz), 5.44 (2H, s), 7.43 (6H, m), 8.22 (1H, d, $J = 8.4$ Hz), 8.67 (1H, d, $J = 2.1$ Hz), 9.38 (1H, br); ^{13}C NMR (100 MHz, $CDCl_3$) δ ppm:

13.88, 20.48, 24.22, 25.60, 28.22, 29.16, 47.61, 47.84, 48.64, 71.48, 109.08, 112.32, 119.16, 122.98, 128.51, 128.74, 128.95, 136.63, 141.31, 143.09, 157.97. MS (EI): *m*/*z* (%) 410 (M^+, 1), 367 (12), 246 (52), 140 (21), 91 (100), 86 (39). Anal. ($C_{23}H_{30}N_4O_3$) C, 67.29; H, 7.37; N, 13.65.

5.4. General method for the preparation of **17** and **18**

A mixture of the corresponding amine (**5** or **6**, 1 equiv) and *m*-chloroperbenzoic acid (4 equiv) in dichloromethane (50 mL/mmol of amine) was heated at reflux for 20 h. The mixture was then evaporated to dryness and treated with aqueous potassium carbonate (5%, 30 mL) and dichloromethane (3 × 30 mL). The combined organic layers were dried ($MgSO_4$) and evaporated to dryness. The desired compound was purified by column chromatography (SiO_2, CH_2Cl_2/MeOH (95:5)).

5.4.1. N-*[5-(3-Benzyloxy-5-nitro-1*H*-indazol-1-yl)-3-oxapentyl]piperidine* N-*oxide* (***17***)

Yield: 72%. ^{1}H NMR (400 MHz, $CDCl_3$) δ ppm: 1.17 (1H, m), 1.35 (2H, m), 1.57 (1H, m), 2.07 (2H, m), 2.77 (2H, t, J = 10.3 Hz), 3.00 (2H, t, J = 11.2 Hz), 3.18 (2H, m), 3.84 (2H, m), 3.97 (2H, m), 4.38 (2H, m), 5.43 (2H, s), 7.29 (1H, d, J = 8.8 Hz), 7.39 (3H, m), 7.52 (2H, m), 8.19 (1H, d, J = 8.8 Hz), 8.64 (1H, s); ^{13}C NMR (100 MHz, $CDCl_3$) δ ppm: 21.27, 22.27, 49.26, 65.06, 66.64, 69.52, 69.80, 71.75, 109.51, 112.37, 118.88, 122.69, 128.52, 128.72, 128.97, 136.52, 141.27, 143.95, 158.09. MS (EI): *m*/*z* (%) 313 (M^+ − 127, 4), 269 (15), 98 (64), 91 (100). IR (KBr, cm^{-1}): 2941, 1614, 1540, 1484, 1329, 1199, 1143, 960. Anal. ($C_{23}H_{28}N_4O_5$) C, 62.71; H, 6.41; N, 12.72.

5.4.2. N,N-*Dimethyl-5-(3-benzyloxy-5-nitro-1*H*-indazol-1-yl)-3-oxapentylamine* N-*oxide* (***18***)

Yield: 40%. ^{1}H NMR (400 MHz, $CDCl_3$) δ ppm: 2.98 (3H, s), 3.44 (2H, t, J = 5.1 Hz), 3.87 (4H, m), 4.37 (2H, t, J = 5.0 Hz), 5.40 (2H, s), 7.28 (1H, d, J = 8.2 Hz), 7.37 (3H, m), 7.50 (2H, m), 8.17 (1H, dd, J = 1.6, 8.2 Hz), 8.60 (1H, d, J = 1.6 Hz); ^{13}C NMR (100 MHz, $CDCl_3$) δ ppm: 46.01, 49.65, 59.03, 59.49, 65.43, 69.62, 69.81, 71.46, 109.91, 112.41, 118.85, 122.79, 128.52, 128.72, 128.93, 136.53, 141.26, 143.86, 158.00. MS (EI): *m*/*z* (%) 313 (M^+ − 87, 3), 91 (82), 71 (30), 58 (100), 44 (11). IR (KBr, cm^{-1}): 2850, 1617, 1540, 1516, 1377, 1329, 1200, 1140, 952, 706. Anal. ($C_{20}H_{24}N_4O_5$) C, 59.99; H, 6.04; N, 13.99.

5.5. General method for the preparation of **19** and **20**

A mixture of the corresponding bromide (**8** or **9**, 1 equiv) and potassium carbonate (1 equiv) in acetonitrile (10 mL/mmol of bromide) was heated at reflux for 28 h. Then, the mixture was evaporated to dryness and treated with aqueous potassium carbonate (5%, 30 mL) and dichloromethane (3 × 30 mL). The combined organic layers were dried ($MgSO_4$) and evaporated to dryness to obtain the desired compound.

5.5.1. 9-Nitro-1,2,4,5-tetrahydro-[1,4,5]oxadiazepino[4,5-a]*indazole-11-one* (***19***)

Yield: 55%. ^{1}H NMR (400 MHz, $CDCl_3$) δ ppm: 4.00 (4H, t, J = 4.2 Hz), 4.24 (2H, m), 4.38 (2H, m), 7.12 (1H, d, J = 9.1 Hz), 8.40 (1H, dd, J = 2.1, 9.1 Hz), 8.81 (1H, d, J = 2.1 Hz); ^{13}C NMR (100 MHz, $CDCl_3$) δ ppm: 46.66, 52.44, 70.27, 70.60, 109.19, 115.67, 122.40, 127.63, 135.93, 146.18, 159.28. MS (EI): *m*/*z* (%) 249 (M^+, 100), 218 (20), 177 (15), 149 (12), 131 (14), 103 (11). Anal. ($C_{11}H_{11}N_3O_4$) C, 53.01; H, 4.45; N, 16.86.

5.5.2. 2-Nitro-7,8,9,10-tetrahydro-[1,2]diazepino[1,2-a]*indazol-12(6*H*)-one* (***20***)

Yield: 60%. ^{1}H NMR (400 MHz, $CDCl_3$) δ ppm: 1.89 (6H, m), 4.13 (2H, m), 4.21 (2H, m), 7.12 (1H, d, J = 9.2 Hz), 8.35 (1H, dd, J = 2.1, 9.2 Hz), 8.81 (1H, d, J = 2.1 Hz); ^{13}C NMR (100 MHz, $CDCl_3$) δ ppm: 28.88, 28.94, 43.45, 49.29, 108.83, 115.00, 122.40, 127.16, 142.00, 144.94, 159.00. MS (EI): *m*/*z* (%) 247 (M^+, 80), 219 (10), 177 (10). Anal. ($C_{12}H_{13}N_3O_3$) C, 58.29; H, 5.30; N, 16.99.

5.6. N,N-*Dimethyl-5-(3-benzyloxy-1*H*-indazol-1-yl)pentylamine* (***22***)

3-Benzyloxy-1-(5-bromopentyl)-1H-indazole (**27**). A mixture of **26** (1 equiv), 1,5-dibromopentane (5 equiv), potassium carbonate (2 equiv) in acetone (10 mL/mmol of **26**) as solvent was heated at reflux for 24 h. After that acetone was evaporated in vacuo and the residue treated with water, brine and chloroform (3 × 30 mL). The combined organic layers were evaporated and added to chromatographic column (SiO_2, $CHCl_3$/MeOH (95:5)) to obtain the intermediate **27** that was used in the next reaction. *N,N-Dimethyl-5-(3-benzyloxy-1H-indazole)pentylamine* (**22**). A mixture of compound **27** (1 equiv) and dimethylamine (5.6 M in ethanol) (2.2 equiv) in ethanol (30 mL/mmol of **27**) was stirred at room temperature for 48 h and then evaporated to dryness. The residue was treated with aqueous sodium hydroxide (0.25 N) and extracted with chloroform (4 × 25 mL). The organic layer was dried with $MgSO_4$ and evaporated in vacuo. ^{1}H NMR (300 MHz, DMSO-d_6) δ ppm: 1.18 (2H, q, J = 7.5 Hz), 1.41 (2H, q, J = 7.5 Hz), 1.75 (2H, q, J = 7.5 Hz), 2.22 (6H, s), 2.31 (2H, t, J = 7.2 Hz), 4.19 (2H, t, J = 6.9 Hz), 5.37 (2H, s), 7.03 (2H, t, J = 7.8 Hz), 7.39 (4H, m), 7.49 (2H, m), 7.59 (1H, d, J = 8.1 Hz); ^{13}C NMR (100 MHz, $CDCl_3$) δ ppm: 24.18, 26.02, 29.29, 44.62, 47.89, 58.71, 70.51, 109.68, 111.74, 119.52, 119.80, 127.69, 127.85, 128.10, 128.52, 137.34, 141.51, 155.03. Anal. ($C_{21}H_{27}N_3O$) C, 74.74; H, 8.06; N, 12.45.

5.7. Biology

5.7.1. Epimastigote culture and growth inhibition assays

T. cruzi epimastigotes, CL Brener clone, were grown at 28 °C in an axenic medium (BHI-tryptose) as previously described, supplemented with 5% fetal bovine serum (FBS) [7,19,28–32]. Cells from a 10-day old culture (stationary phase) were inoculated into 50 mL of fresh culture medium to give an initial concentration of 1 × 10^6 cells/mL. Cell growth was followed by measuring everyday the absorbance of the culture at 600 nm. Before inoculation, the media were supplemented with the indicated amount of the drug from a stock solution in DMSO. The final concentration of DMSO in the culture media never exceeded 0.4% and the control was run in the presence of 0.4% DMSO and in the absence of any drug. No effect on epimastigotes' growth was observed in the presence of up to 1% DMSO in the culture media. The percentage of inhibition was calculated as follows: $\% = \{1 - [(A_p - A_{0p})/(A_c - A_{0c})]\} \times 100$, where $A_p = A_{600}$ of the culture containing the drug at day 5; $A_{0p} = A_{600}$ of the culture containing the drug just after addition of the inocula (day 0); $A_c = A_{600}$ of the culture in the absence of any drug (control) at day 5; $A_{0c} = A_{600}$ in the absence of the drug at day 0. To determine IC_{50} values, 50% inhibitory concentrations, parasite growth was followed in the absence (control) and presence of increasing concentrations of the corresponding drug. At day 5, the absorbance of the culture was measured and related to the control. The IC_{50} value was taken as the concentration of drug needed to reduce the absorbance ratio to 50%.

5.7.2. Trypomastigotes and viability assay

VERO cells were infected with SN-3 strain of *T. cruzi* metacyclic trypomastigotes from 15 days old epimastigote cultures. Subsequently, the trypomastigotes harvested from this culture were used to reinfect further VERO cell cultures at 1 × 10^6 parasites per 25 cm^2 density. VERO cell cultures infected with trypomastigotes were incubated at 37 °C in humidified air and 5% CO_2 for 5–7 days. After that time, the culture medium was collected, centrifuged at 3000*g*

for 5 min, and the trypomastigote-containing pellet was resuspended in RPMI supplemented with fetal bovine serum 5% and penicillin–streptomycin at a final density of 1×10^7 parasites/mL. 210×10^6 trypomastigotes are equivalent to 1 mg of protein or 12 mg of wet weight.

Viability assays were performed using the MTT reduction method as described previously [34]. 1×10^7 trypomastigotes were incubated in FBS-RPMI culture medium at 37 °C for 24 h with or without the studied compounds. An aliquot of the parasite suspension was extracted and incubated in a 96-flat bottomed well plate and MTT was added at 0.5 mg/mL final concentration, incubated at 28 °C for 4 h and then made soluble with 10% SDS–0.1 mM HCl and incubated overnight. Formazan formation was measured at 570 nm with reference wavelength at 690 nm in a multiwell reader (Labsystems MultoskanMS, Finland). Untreated parasites were used as negative controls (100% of viability).

5.8. Cyclic voltammetry

In protic media, the solutions were prepared starting from a stock solution 0.1 M of sample, 5-NI, in DMSO. The final solution was prepared through corresponding dilution to obtain a sample with final concentration, on the voltammetric cell, of 1.0 mM. Experiments were run in buffer Britton–Robinson/EtOH (70:30) and 0.1 M of KCl, at different pH, which were used for the dilutions. The pH was previously adjusted adding small amounts of concentrated NaOH or HCl, depending on the desired final pH. CV was carried out using a Metrohm 693VA instrument with a 694VA Stand convertor and a 693VA Processor, under a nitrogen atmosphere at room temperature, using a three-electrode cell. A hanging mercury drop electrode was used as the working electrode, a platinum wire as the auxiliary electrode, and saturated calomel (SC) as the reference electrode.

5.9. ESR experiments

ESR spectra were recorded in the X-band (9.7 GHz) using a Bruker ECS 106 spectrometer with a rectangular cavity and 50 kHz field modulation. The hyperfine splitting constants were estimated to be accurate within 0.05 G. ESR spectra were produced using a microsomal fraction (6 mg protein/mL) obtained from *T. cruzi*, in a reaction medium containing 1 mM NADPH, 100 mM DMPO, in 20 mM phosphate buffer, pH 7.4. All experiments were done after 15 min of incubation at 28 °C of 5-NI with *T. cruzi* microsomal fraction, NADPH and DMPO in an aerobic environment. The ESR spectra were simulated using the program WINEPR Simphonia 1.25 version.

Parasites for ESR studies. *T. cruzi* epimastigotes (Tulahuen strain), from our collection, were grown at 28 °C in Diamond's monophasic medium as reported earlier, with blood replaced by 4 mM hemin [16,17]. Fetal calf serum was added to a final concentration of 4%. Parasites: 8×10^7 cells correspond to 1 mg protein or 12 mg of fresh weight.

5.10. Crystallography study

The crystal and molecular structures of derivative **13**, $C_{20}H_{24}N_4O_4$, have been determined by X-ray diffraction methods. The substance crystallizes in the triclinic *P*-1 space group with $a = 9.303(1)$, $b = 10.037(2)$, $c = 10.773(2)$ Å, $\alpha = 113.89(1)$, $\beta = 96.84(1)$, $\gamma = 108.25(1)^\circ$, and $Z = 2$ molecules per unit cell. The structure was solved from 2689 reflections with $I > 2\sigma(I)$ and their non-H atoms refined anisotropically by least squares. The hydrogen atoms were located in a difference Fourier map and refined isotropically at their found positions. The final agreement *R*1 factor is 0.048. Intramolecular bond distances and angles, along with other crystallographic data, are given as Supporting information. Crystallographic data (excluding structure factors) for the structure in this paper have been deposited at the Cambridge Crystallographic Data Centre as supplementary publication number CCDC-683743. Copies of the data can be obtained, free of charge, on application to CCDC, 12 Union Road, Cambridge CB2 1EZ, UK [fax: 144-(0)1223-336033 or e-mail: deposit@ccdc.cam.ac.uk].

Acknowledgements

Financial support from PEDECIBA (Uruguay), CICYT (Spain, project SAF 2006-04698) and Collaborative Projects FONDECYT 1071068/7070282, Consejo Superior de Investigaciones Científicas (Spain) 2006CL0035 CSIC 16/07-08, MECESUP UMC-0204 and CONICET (Argentina) is acknowledged. The authors thank RTPD network and MECESUP UCH-0408 for the scholarship to J.R. and PEDECIBA-QUÍMICA for a scholarship to A.G. O.E.P. is a research fellow of CONICET. Proyecto Anillo ACT 29 CONICYT/PBCT; Proyecto Bicentenario Red 07, FONDECYT 1061072.

Appendix. Supporting information

Crystal data and structure solution methods and refinement results for derivative **13** (Table S1), listings of atomic fractional coordinates and equivalent isotropic parameters (Table S2), full intramolecular bond distances and angles (Table S3), anisotropic displacement parameters (Table S4) and hydrogen atoms' positions and isotropic displacement parameters (Table S5) are provided. Supplementary data associated with this article can be found in the online version, at doi:10.1016/j.ejmech.2008.07.018.

References

[1] World Health Organization (OMS), Report of the Scientific Working Group on Chagas Disease, Buenos Aires, Argentina, 2005.
[2] H. Ferreira, Rev. Soc. Bras. Med. Trop. 23 (1990) 209–211.
[3] S. Cuzzocrea, D.P. Riley, A.P. Caputi, D. Salvemini, Pharmacol. Rev. 53 (2001) 135–159.
[4] W.H. Koppenol, Free Radic. Biol. Med. 15 (1993) 645–651.
[5] H. Cerecetto, M. Gonzalez, Curr. Top. Med. Chem. 2 (2002) 1187–1213.
[6] J.D. Maya, S. Bollo, L.J. Nunez-Vergara, J.A. Squella, Y. Repetto, A. Morello, J. Perie, G. Chauviere, Biochem. Pharmacol. 65 (2003) 999–1006.
[7] (a) V.J. Aran, C. Ochoa, L. Boiani, P. Buccino, H. Cerecetto, A. Gerpe, M. Gonzalez, D. Montero, J.J. Nogal, A. Gomez-Barrio, A. Azqueta, A.L. de Cerain, O.E. Piro, E.E. Castellano, Bioorg. Med. Chem. 13 (2005) 3197–3207;
(b) L. Boiani, A. Gerpe, V.J. Arán, S. Torres de Ortiz, Elva Serna, N. Vera de Bilbao, L. Sanabria, G. Yaluff, H. Nakayama, A. Rojas de Arias, J.D. Maya, J.A. Morello, H. Cerecetto, M. González, Eur. J. Med. Chem. (2008). doi:10.1016/j.ejmech.2008.06.024.
[8] C. Olea-Azar, H. Cerecetto, A. Gerpe, M. Gonzalez, V.J. Aran, C. Rigol, L. Opazo, Spectrochim. Acta Part A – Mol. Biomol. Spectrosc. 63 (2006) 36–42.
[9] V.J. Aran, J.L. Asensio, J.R. Ruiz, M. Stud, J. Chem. Soc., Perkin Trans. 1 (1993) 1119–1127.
[10] L. Baiocchi, G. Corsi, G. Palazzo, Synthesis (Stuttg) (1978) 633–648.
[11] J. Schmutz, W. Michaelis, F. Hunziker, Helv. Chim. Acta 47 (1964) 1986.
[12] S.D. Wyrick, P.J. Voorstad, G. Cocolas, I.H. Hall, J. Med. Chem. 27 (1984) 768–772.
[13] P. Bruneau, C. Delvare, M.P. Edwards, R.M. McMillan, J. Med. Chem. 34 (1991) 1028–1036.
[14] S. Bollo, L.J. Nunez-Vergara, C. Barrientos, J.A. Squella, Electroanalysis 17 (2005) 1665–1673.
[15] P. Zuman, J. Electroanal. Chem. 168 (1984) 249–260.
[16] I. Rubinstein, J. Electroanal. Chem. 183 (1985) 379–386.
[17] S. Bollo, L.J. Nunez-Vergara, M. Bonta, G. Chauviere, J. Perie, J.A. Squella, Electroanalysis 13 (2001) 936–943.
[18] S. Bollo, L.J. Nunez-Vergara, J.A. Squella, J. Electroanal. Chem. 562 (2004) 9–14.
[19] A. Gerpe, G. Aguirre, L. Boiani, H. Cerecetto, M. Gonzalez, C. Olea-Azar, C. Rigol, J.D. Maya, A. Morello, O.E. Piro, V.J. Aran, A. Azqueta, A.L. de Cerain, A. Monge, M.A. Rojas, G. Yaluff, Bioorg. Med. Chem. 14 (2006) 3467–3480.
[20] C. Olea-Azar, C. Rigol, L. Opazo, A. Morello, J.D. Maya, Y. Repetto, G. Aguirre, H. Cerecetto, R. Di Maio, M. Gonzalez, W. Porcal, J. Chil. Chem. Soc. 48 (2003) 77–79.
[21] C. Olea-Azar, C. Rigol, F. Mendizabal, A. Morello, J.D. Maya, C. Moncada, E. Cabrera, R. di Maio, M. Gonzalez, H. Cerecetto, Free Radic. Res. 37 (2003) 993–1001.
[22] C.S. Lai, T.A. Grover, L.H. Piette, Arch. Biochem. Biophys. 193 (1979) 373–378.

[23] C. Olea-Azar, C. Rigol, F. Mendizabal, R. Briones, Mini Rev. Med. Chem. 6 (2006) 211–220.
[24] S.N.J. Moreno, R. Docampo, R.P. Mason, W. Leon, A.O.M. Stoppani, Arch. Biochem. Biophys. 218 (1982) 585–591.
[25] R. Docampo, A.O.M. Stoppani, Arch. Biochem. Biophys. 197 (1979) 317–321.
[26] M. Masana, E.G.D. Detoranzo, J.A. Castro, Biochem. Pharmacol. 33 (1984) 1041–1045.
[27] J.D. Maya, Y. Repetto, M. Agosin, J.M. Ojeda, R. Tellez, C. Gaule, A. Morello, Mol. Biochem. Parasitol. 86 (1997) 101–106.
[28] H. Cerecetto, R. Di Maio, M. Gonzalez, M. Risso, P. Saenz, G. Seoane, A. Denicola, G. Peluffo, C. Quijano, C. Olea-Azar, J. Med. Chem. 42 (1999) 1941–1950.
[29] G. Aguirre, H. Cerecetto, R. Di Maio, M. Gonzalez, W. Porcal, G. Seoane, M.A. Ortega, I. Aldana, A. Monge, A. Denicola, Arch. Pharm. 335 (2002) 15–21.
[30] G. Aguirre, M. Bolani, H. Cerecetto, A. Gerpe, M. Gonzalez, Y.F. Sainz, A. Denicola, C.O. de Ocariz, J.J. Nogal, D. Montero, J.A. Escario, Arch. Pharm. 337 (2004) 259–270.
[31] G. Aguirre, L. Boiani, H. Cerecetto, R. Di Maio, M. Gonzalez, W. Porcal, A. Denicola, M. Moller, L. Thomson, V. Tortora, Bioorg. Med. Chem. 13 (2005) 6324–6335.
[32] G. Aguirre, L. Boiani, M. Boiani, H. Cerecetto, R. Di Maio, M. Gonzalez, W. Porcal, A. Denicola, O.E. Piro, E.E. Castellano, C.M.R. Sant'Anna, E.J. Barreiro, Bioorg. Med. Chem. 13 (2005) 6336–6346.
[33] M.O.F. Khan, Drug Target Insights 2 (2007) 129–146.
[34] S. Muelas-Serrano, J.J. Nogal-Ruiz, A. Gómez-Barrio, Parasitol. Res. 86 (2000) 999–1002.